Effect of Cd2+ Cations on AC Conductivity of Stearic Acid Metal-Insulator-Semiconductor Diode

Syed A Malik[1, a*)] and Asim K Ray[2, b)]

[1]*Department of Physics, Universiti Pendidikan Sultan Idris, 35900 Tanjong Malim, Malaysia*
[2]*Department of Electronic and Computer Engineering, Brunel University, Uxbridge, London, UB8 3PH, UK*

[a*)]syed.malik@fsmt.upsi.edu.my
[b)]Asim.Ray@brunel.ac.uk

Abstract. We report on observations of the effect of Cd^{2+} ions on the AC electrical properties of stearic acid (SA) thin films in metal-insulator-semiconductor (MIS) diode-like structure. The MIS structure was fabricated using 40-layers Langmuir-Blodgett (LB) films of stearic acid (SA) on hydrophobic n-type silicon (n-Si) substrates. Cadmium sulphide (CdS) nanoparticles were embedded inside the SA matrix by exposure to H_2S gas for a period of 12 hours. The frequency dependence of capacitance (C-f), conductance (G-f) and $\tan\delta$ characteristics of the Al/SA/Si structures were investigated in dark at room temperature. The capacitance for LB film of stearic acid with Cd^{2+} ions showed almost no frequency dependence. However, the device containing CdS nanoparticles exhibited strong frequency dependencies at frequencies greater than 100 kHz. The variation in the capacitance of the device as a function of modulating frequency was due to the polarization of the dielectric medium in which positive and negative charges were displaced with respect to their equilibrium positions. The conductance measurement (G-f) shown similar result which translated this to the increase in relaxation time. Futhermore, the dielectric loss ($\tan\delta$) measurement of SA+CdS device showed the increase in power losses as a function of frequency for both devices. The series resistance is believed to be dominant in the higher frequency range since the LB film resistance (R_{LB}) decreases with frequency.

INTRODUCTION

Silicon wafer is extensively dominating the microelectronics industry due to its mature technology, making it technologically an important substrate [1]. By coating monolayers of organic thin films directly on top of the silicon surface, the new created electronic devices can be tuned through precise control of the insulating layers. Fundamental to the application of organic films in electronic devices is the static and dynamic electrical properties of the monolayers. Metal-insulator-semiconductor (MIS) structures have been widely investigated due to their major applications in semiconductor devices. Their significant feature that they have storage layer property, capacitance effect and high-k dielectric constant. The MIS electronic devices can be produced by using a hybrid organic-inorganic composite film as the dielectric material which offers a wide range of interesting applications especially in electronics and optoelectronics. The importance of MIS Schottky diodes entrenched in their importance of the insulating layer embedded between metal and semiconductor [1]. The presence of a dielectric material between two conductors gives the device the electrical properties of a diode (or capacitor). The existence of such boundary layer give sturdy control on the device capacitance and conductance

characteristics against the operating frequencies. The DC and AC electrical measurements are one of the most useful ways to probe the quality of both dielectric and the insulator-semiconductor interface.

Owing to the various technologies available nowadays in depositing insulating layers of the MIS structure, a complete understanding of its electrical properties of different processing technology is of great concern. The organic materials can be deposited by using the conventional dry method such as molecular beam epitaxy (MBE), and sputtering technique. MBE is a highly sophisticated and precise technique used for the deposition of thin film and inorganic nanoparticles. However, it is very costly. An alternative technology is by using low cost wet technology such as chemical bath deposition, electrodeposition, spin-coating and Langmuir-Blodgett (LB). Out of these, the LB technique has proved to be the most promising method for the preparation of organic thin films [2]. This is primarily due to their variable layer architecture with a high degree of molecular order and the exact control of the film thickness [3]. It has the benefit that high vacuum and elevated temperatures are not required, and film thicknesses are easily derived from the number of layers deposited [4]. This paper is set as a completion to our previous work on the MIS device of LB film incorporating Cd2+ ions which focused on DC current-voltage [5], 1/f noise [6, 7] and capacitance-voltage [8].

METHODOLOGY

The fabrication of MIS structures involved careful preparation of silicon (Si) substrates, deposition of thin organic film and electrical contacts. The fabrication of device was performed in a class 100 clean room environment following carefully drawn up procedures including health and safety guidelines. The methods for device fabrication involved etching and cleaning of silicon substrates, preparation of the LB trough, LB film deposition, and metal contact deposition. Substrates in this investigation were n-type silicon wafers (100). The thickness and resistivity (ρ) were approximately 300 μm and 4.5 Ω.cm, respectively. As part of the device requirements, silicon dioxide (SiO_2) layers with thickness in the range of 0.8 μm to 1.5 μm were thermally grown on top of the silicon wafers. The wafers were then cut to the dimension of a glass slide which was approximately 76 mm x 26 mm. A part of the SiO_2, approximately 15 mm, was then etched in a mix of hydroflouric (HF) acid and Millipore water (18 MΩ.cm) with a moderate concentration ratio of 1:5, resulting in 15 mm width of the bare silicon substrate.

A PC-controlled Langmuir-Blodgett trough (model 622D2) from Nima Technology Ltd., UK with a total trough volume of approximately 1.4 liter was used in this work. The trough was cleaned thoroughly by using chloroform and propanol with dust-free wipes (Kimberly-Clark) which are recommended for an LB trough. The water used for subphase is purified Mili-Q water of resistivity of about 18 MΩ.cm and pH value of 5.5. Cadmium chloride solution with concentration of 0.1 mol/l was prepared by dissolving 18.3 g of $CdCl_2$ salt into 1 liter of water. An amount of 6 ml of the solution was mixed thoroughly into the subphase and a $CdCl_2$ solution was produced with a concentration of approximately $5x10^{-4}$ M. The molecular weight of $CdCl_2$ is 183.3 g/mol.

Monolayers of stearic acid molecules were formed by carefully spreading 80 μl of its solution drop by drop, at different places onto the surface of water subphase. The concentration of the stearic acid solution was 1 mg/ml in chloroform. Cadmium chloride salt, chloroform and stearic acid were of high purity grade. A period of 20 - 30 minutes was found to be sufficient for the evaporation of any residual solvent to take place prior to the compression of the barriers. The surface of the subphase was visually monitored and contaminations on the surface were removed by siphoning using a vacuum pump, prior to the spreading of stearic acid solution.

The film deposition took place at room temperature and the pH of the subphase was held at 5.5. The monolayer was compressed at a target pressure of 28 mN/m and the pressure was maintained at that level throughout the deposition process. Dipping speeds for downward and upward strokes were set to 15 mm/min and 20 mm/min respectively, with a 3 minutes time interval to allow sufficient drying of the film. Forty monomolecular layers of LB film of stearic acid (SA) molecules were transferred from the subphase onto the n-type silicon substrate by the vertical dipping method. This required spreading stearic acid solution several times onto the water surface. The thickness of the film was estimated to be 100nm due to the fact that monolayer thickness of stearic acid is approximately 2.5 nm [9].

Using an Edwards E306A thermal evaporator, aluminum electrodes were deposited on top of the LB film surface (top contact) and on the back of the silicon substrate (bottom contact). The procedure for metal contact deposition started with placing the metal source on a tungsten filament. The evaporation chamber was then pumped down to a pressure lower than 2×10^{-5} mbar .When sufficiently large current is passed through the filament, the metal sublimed onto the target substrate above the source, producing a thin metal film. The thickness of the contacts and the rate of coating were both monitored in-situ by using a quartz crystal microbalance (QCM).

The films investigated in this study were insulating LB films of stearic acid transferred from the sub-phase containing metallic cadmium (Cd^{2+}) cations. Composite LB films were deposited onto n-type silicon substrate and metal-insulator-semiconductor (MIS) device structure was fabricated containing these stearic acid films and referred as "SA" device. Some LB films of composite stearic acid were then treated with hydrogen sulphide (H_2S) gas in order to embed cadmium sulphide (CdS) nanoparticles into the SA matrix and named as "SA+CdS" device. The fabricated LB film of cadmium stearate (CdSt2) in MIS structure device is shown in figure 1.

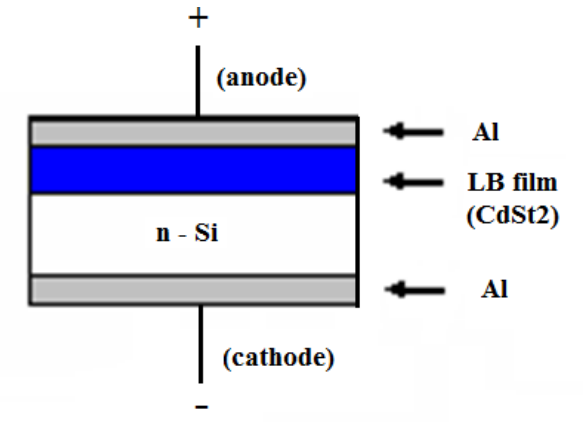

FIGURE 1. Fabricated MIS diode.

AC CONDUCTIVITY MEASUREMENT

The electrical admittance (or impedance) spectroscopy is one of the most important non-destructive methods for obtaining information in the bulk and on the interfacial regions between semiconductor and dielectric medium of any kind of solid or liquid material [2]. By applying an electrical field perpendicular to the surface (known as field effect), the occupancy of surface states in semiconductors can be varied which in turn will change the physical quantities of the devices i.e. capacitance and conductance.

Impedance spectroscopic measurement setup as shown in figure 3 was used to measure capacitance (C) and conductance (G) simultaneously as a function of frequency (C-f and G-f). Prior to measurement the LCR meter was calibrated for conductor cables used in connecting the samples by using an open and short-circuit test.

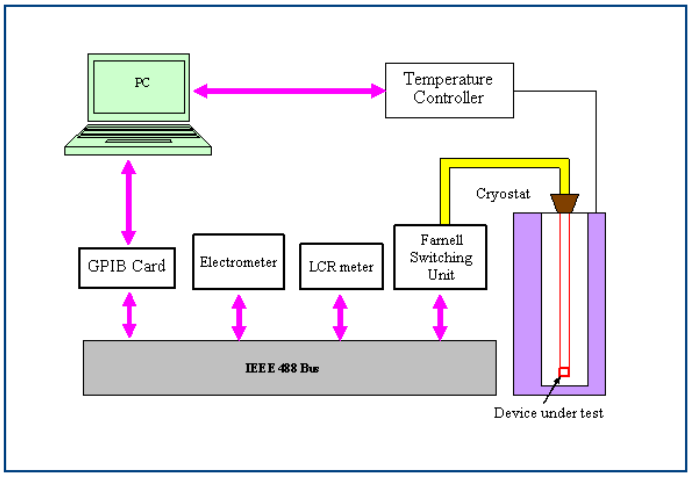

FIGURE 3. Schematic diagram of a complete AC and DC electrical impedance/conductance measurement system

RESULTS AND DISCUSSION

Admittance measurements

The admittance ($Y = G \pm jB$ *or* $Y = \sigma' \pm j\sigma''$) of the MIS device was measured as a function of frequency by applying a sinusoidal voltage signal and monitoring the amplitude and phase shift of the resulting current. As a result the data obtained from these measurements are a complex presentation, the real (σ') and imaginary parts (σ") of the admittance. The frequency was swept from 20Hz to 1MHz in a logarithmic scale. The measurements were performed in the dark at room temperature. The amplitude of the AC signal voltage was $20mV_{rms}$ with DC bias voltage set to zero. Since DC bias voltage is zero, the effect of DC leakage current on capacitance can be ignored.

Figure 4 shows the variation of capacitance (C) and the frequency normalized conductance (G/ω) of the device (SA and SA+CdS) measured at room temperature. In order to compare their results, both C and G/ω are normalized to device area (C/A and G/ωA). As previously observed in C-V measurements by embedding the LB film of stearic acid with CdS nanoparticles, the device capacitance increased due to the increase in dielectric constant as seen previously by C-V measurement [8]. As can be seen, the capacitance for LB film of stearic acid with Cd^{2+} ions showed almost no frequency dependence. This was similar to the result of LB films of cadmium arachidate measured at room temperature [10].

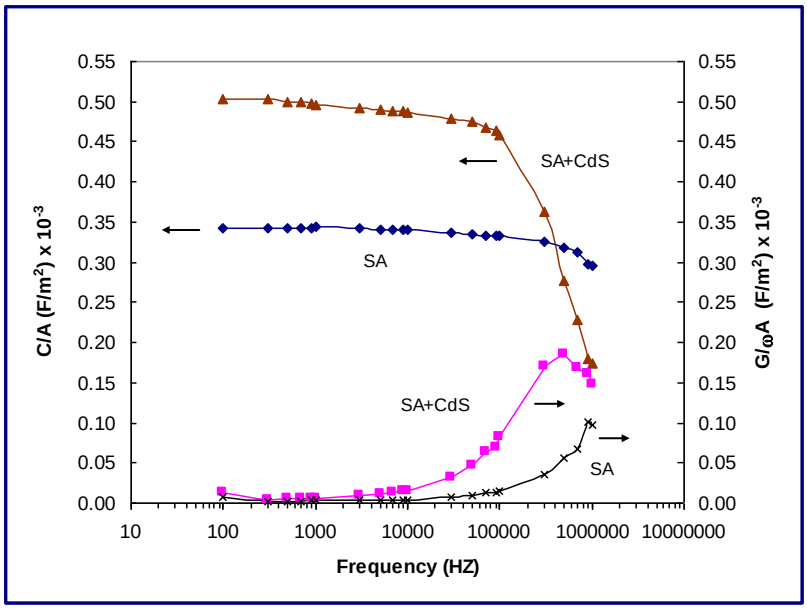

FIGURE 4. Capacitance and normalized conductance per unit area as a function of frequency.

On the contrary, the sample containing CdS nanoparticles exhibited strong frequency dependencies at frequencies greater than 100 kHz. Below this, the capacitance was less dependent on the signal frequency which is similar in behavior to SA. For SA+CdS the capacitance went from a high value, at the low frequency plateau (Cs), to the low value of high frequency. Since the maximum sweep frequency of the HP 4284A LCR meter was only1 MHz, the high frequency plateau in capacitance (C_∞) was not observed. It was found that by embedding CdS nanoparticles in stearic acid matrix, the capacitance of LB films increased primarily

The variation in the capacitance of the device as a function of modulating signal frequency was due to the polarization of the dielectric medium in which positive and negative charges were displaced with respect to their equilibrium positions [11]. From the graph, the normalized conductance (G/ωA) of the SA+CdS device shows a peak at 500 kHz. No peak was observed for SA devices within the range of investigation. The relaxation time (τ) due to the induced dipole moments for SA+CdS device was estimated to be 2 μs whilst SA devices are believed to have smaller relaxation time. The increase in relaxation time was believed to be due to the increase in dielectric constant of the LB films when CdS nanoparticles were embedded in the strearic acid matrix.

The electrical conductivity of many different dielectric materials was known to depend on the modulating signal frequency. Jonscher has observed a similar pattern of AC conductivity behavior of different dielectric on modulating signal frequency and later proposed a universal dielectric response model which is represented by $(\omega)\alpha\ \omega^n$, where $n \leq 1$ [12]. Figure 5 shows the AC conductivity of the devices as a function of frequency at room temperature. In contrast to the capacitance (figure 4), the conductance shown a different behavior; increasing with the modulating frequency. For low signal frequency (below 1 kHz), the universal law is followed by the exponential constant n ~ 0.8.

This type of dependence agrees well with the prediction model describing hopping transport mechanism [13]. Deviation from Jonscher's universal law was seen in signal frequency greater than 1 kHz. For frequencies up to 100 kHz the exponential constant was found to be greater than unity with n ~ 1.6. Since n is close to 2, it suggests a power law agreement, that is, this was due to the dominance of series resistance (Rs) which is associated with the neutral region of the semiconductor between the depletion region and bottom contact [14] and also from the electrode contacts. As conductance of a device is a representation of losses in the material, it shows that power losses in both devices are highly dependent on the signal frequency.

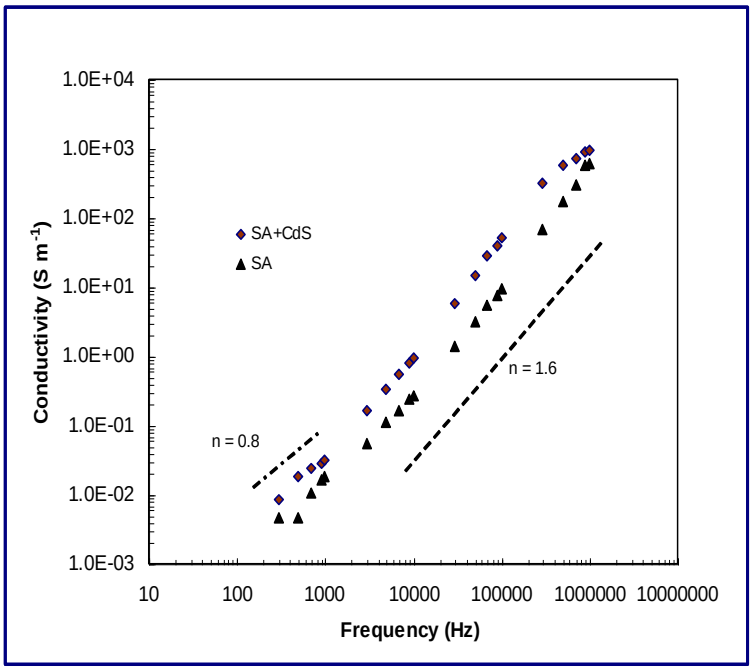

FIGURE 5. AC conductivity versus modulating frequency for both devices.

Figure 6 shows the dissipation factor, also known as dielectric loss $(\tan\delta)$ of SA and SA+CdS devices as a function of modulating signal frequency measured in the dark at room temperature. As can be seen, the dielectric loss is highly dependent on the modulating signal frequency. A minimum in $\tan\delta$ is apparent over the frequency range investigated with a narrow-band curve. The dielectric loss decreases with increases in frequency till the loss minimum $(\tan\delta_{min})$ is observed and thereafter, tan δ increases linearly with frequency$(\tan\delta \infty f)$. These results agree well with a model by Goswami and Goswami [15] which explain the variation of tan δ with frequency and the appearance of $\tan\delta_{min}$ in the audio range frequency. The resulting curve is similar to the band-pass filter response of a varactor diode [16] which, suggests that the LB film of stearic acid cannot be modelled by a simple film resistance R_{LB} and capacitance C_{LB} in parallel with each other. The electrodes are assumed to contribute a resistance Rs in series with the sample as modelled by a three-element model reported earlier [5].

Also as can be seen from the graph, the SA+CdS device has slightly larger dielectric loss when compared to the SA one. This could be due to CdS nanoparticles formed in the stearic acid matrix which are believed to act as carrier traps. This comparison is in agreement with the finding of lower leakage current in SA+CdS devices as discovered previously in the I-V measurements. In general, the magnitude of dielectric loss for both devices was found to be falling for the most part of the interval $0.007 < \tan\delta < 1$ (or $0.4^o < \delta < 45^o$ with minimum dielectric loss

($tan\ \delta_{min}$) appeared at minimum frequency ($f_{min} = \frac{\omega_{min}}{2\pi}$) of approximately $1kHz$ and $2\ kHz$ for SA and SA+CdS devices respectively. The series resistance was dominant in the higher frequency range since the LB film resistance (R_{LB}) decreases with frequency. The effect was a large dielectric loss at high frequencies.

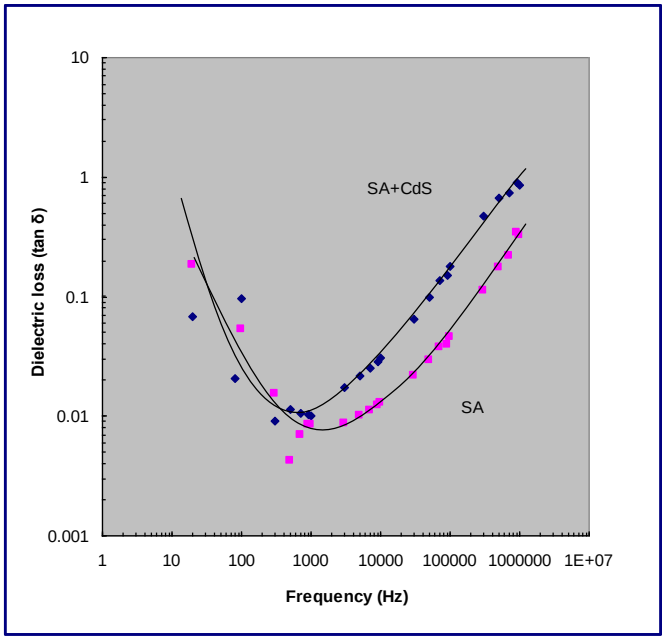

FIGURE 6. Dielectric loss for SA and SA+CdS devices measured at room temperature

–CONCLUDING REMARKS

The capacitance for LB film of stearic acid with Cd^{2+} ions showed almost no frequency dependence. However, the device containing CdS nanoparticles exhibited strong frequency dependencies at frequencies greater than 100 kHz. The decrease of capacitance with increasing frequency is called anomalous frequency dispersion. This type of behavior is generally caused by the creation of higher density of surface states at the interface between insulator and semiconductor. Also, frequency dispersion might arise from the series resistance from low substrate doping. The typical MIS behavior was not observed at a higher modulating frequency (1 MHz). This showed that interface traps were no longer able to follow the probing AC signal in the high-frequency regime. In contrast to the capacitance, the conductance shown a different behavior; increasing with the modulating frequency. The series resistance was dominant in the higher frequency range since the LB film resistance decreases with frequency. The effect was a large dielectric loss at high frequencies.

REFERENCES

(1) Bathaei, N., Weng, B. B, & Sigmarsson, H., Materials Science in Semiconductor Processing., 96 73-77 (2019)
(2) Jonscher, A. K. J. Phys. D: Appl. Phys. 32(14), R57 (1999)

1. Prasanna Lakshmi, B., Rajagopal Reddy, & V., Janardhanam, V., Appl. Phys. A, **113**:713, (2013).
2. Wenyao Yang, Jianhua Xu, Yunwu Mao, Yajie Yang & Yadong Jiang, Synthesis and Reactivity in Inorganic, Metal-Organic, and Nano-Metal Chemistry, **46**(5), 735-740, (2016).

3. Ray A.K., (2017), Organic Materials for Chemical Sensing. In: Kasap S., Capper P. (eds) Springer Handbook of Electronic and Photonic Materials. Springer Handbooks. Springer, Cham.
4. Gould R.D., Kasap S., Ray A.K., (2017), Thin Films. In: Kasap S., Capper P. (eds) Springer Handbook of Electronic and Photonic Materials. Springer Handbooks. Springer, Cham.
5. Malik S., Ray Hassan A. K.,, Nabok, A. V. IEEE transactions on nanotechnology **2**(3), 149-153, 2003.
6. Malik S, Ray A. K.,, S Bruce, Semiconductor science and technology **20**(5), 453, (2005).
7. SA Malik S, Ray A. K.,, 10th IEEE International Conference on Nanotechnology, 413-416, (2010).
8. S Malik S, Ray A. K.,, FH Naning, IOP Conference Series: Materials Science and Engineering **380**(1), 012003, (2018).
9. Petty M.C.: *Langmuir–Blodgett Films: An Introduction*, (Cambridge Univ. Press, Cambridge 1996).
10. Çapan R., Richardson T. , Hassan A.K., Davis Frank, Materials Chemistry and Physics, **143**(3), 1258-1264, (2014).
11. Kasap S.O., *Principles of Electrical Engineering Materials and Devices*, (McGraw-Hill, New York, 1997).
12. Jonscher A.K., Nature, **267**, 673-679, (1977).
13. Petty M.C., Pearson C., Monkman A.P, Casalini R., Capaccioli S., and Nagel J., Colloid Surface A, **171**(1-3), 159-166, (2000).
14. Rhoderick E.H., and Williams R.H., *Metal–Semiconductor Contacts*, 2nd ed., (Clarendon Press, Oxford, 1988).
15. Goswami A., and Goswami Amit P., **16**, 175-185, (1973).
16. Sze S.M., *Physics of Semiconductor Devices*, 3rd. ed., (John Wiley & Sons, New York, 2006).